2013 American Control Conference (ACC)
Washington, DC, USA, June 17-19, 2013

The Price of Synchrony: Resistive Losses due to Phase Synchronization in Power Networks

Bassam Bamieh and Dennice F. Gayme

Abstract— **We investigate the total resistive losses incurred in returning a power network of identical generators to a synchronous state following a transient stability event or in maintaining this state in the presence of persistent stochastic disturbances. We formulate this cost as the input-output H^2 norm of a linear dynamical system with distributed disturbances. We derive an expression for the total resistive losses that scales with the size of the network as well as properties of the generators and power lines, but is independent of the network topology. This topologically invariant scaling of what we term the price of synchrony is in contrast to typical power system stability notions like rate of convergence or the region of attraction for rotor-angle stability. Our result indicates that highly connected power networks, whilst desirable for higher phase synchrony, do not offer an advantage in terms of the total resistive power losses needed to achieve this synchrony. Furthermore, if power flow is the mechanism used to achieve synchrony in highly-distributed-generation networks, the cost increases unboundedly with the number of generators.**

I. Introduction

Changes to the electric power grid are being driven by many factors such as increased demand, renewable energy mandates [1] and further deregulation of the industry [2], [3]. The new grid will have to deal with higher levels of uncertainty from renewable energy sources, changing load patterns and increasingly distributed energy generation. These changes are likely to make it more prone to stability issues. In particular, they have the potential to create problems associated with rotor-angle stability, which is the ability of the power grid to recover synchrony after a disturbance [4]. Synchrony refers to the condition when both the frequency and phase of all generators within a particular power network are aligned. Loss of synchrony can lead to load shedding.

A special case of rotor-angle stability is the so-called transient stability problem, which is associated with large angle disturbances due to events such as generator, power line or other component failures. Such abrupt changes can also be caused by the intermittent behavior of renewable energy sources. There is a large body of transient stability literature, see e.g. [5], [6]. Most of this work focuses on the existence of Lyapunov like energy functions [7], [8] and their use in determining a region of attraction type criteria for a particular synchronous state or set of states, e.g. [9], [10].

B. Bamieh is with the Department of Mechanical Engineering at the University of California at Santa Barbara, Santa Barbara, CA, USA, 93106. (bamieh@engineering.ucsb.edu)
D. F. Gayme is with the Department of Mechanical Engineering at the Johns Hopkins University, Baltimore, MD, USA, 21218. (dennice@jhu.edu).
This work is partially supported by AFOSR (FA9550-10-1-0143) and NSF (ECCS 1230788).

A recent research trend has been to draw connections between problems in distributed system control and power network stability. This literature is vast, but we note in particular a series of works that use a set of coupled Kuramoto oscillators to represent the power network [11], [12]. This non-uniform Kuramoto oscillator modeling framework uses a first order approximation of the network reduced classical power system model to provide network parameter dependent analytical conditions for frequency and phase synchronization [12]. Similar first order models have been employed to investigate how power flow scheduling and adding more power lines (i.e., increasing graph connectivity) affects the rate of convergence in a power network [13].

In the present paper, we examine the connections between distributed control systems and power network stability in a different context. We do not study stability, but rather assume that the network will return to a synchronized state after disturbances. Instead we focus on the cost of keeping the network in synchrony, i.e. how much real power is required to drive the system to a stable, synchronous operating condition. Lack of synchrony leads to circulating currents [14] passing between generators whose angles are out of phase. This flow of current leads to resistive power losses over the power lines due to their non-zero line resistances. This loss is generally considered relatively small compared to the total real power flow in a typical power network. It is however unclear whether these losses will be small in power grids of the future, which are expected to have highly distributed generation, and consequently many more (though typically smaller power capacity) generators than today's grid.

The problem that is analyzed is that of a large network of many identical generators. We consider several scenarios such as the power network encountering disturbance (transient stability) events, or being subjected to persistent stochastic disturbances where the system is continuously correcting for these disturbances. In both of these scenarios, we quantify the total power lost due to non-zero line resistances. Our main result, in equation (13), shows that this power loss scales with the product of the *network size* and the *ratio of line resistances to their reactances* (which is assumed to be the same for all links). The latter quantity is normally assumed to be rather small [15]. However, this result shows that even though that ratio is small, the proportionality with the number of generators indicates that resistive losses may become significant in large networks. Furthermore, and perhaps more surprisingly, these losses are independent of the network topology, i.e. highly connected or loosely connected networks incur the same resistive power

978-1-4799-0178-4/$31.00 ©2013 AACC

losses in recovering synchrony.

Our results indicate that the cost of maintaining synchrony (using power flows) is essentially a function of the number of generators in the network and not of its topology. We should point out that this conclusion is not inconsistent with other results on power system stability and performance measures. For example, interaction strength and network topology play important roles in determining whether a system can synchronize [7], [11], [12], [16] and the rate of convergence or damping of a power system is directly related to the network connectivity [13]. The numerical examples we present in this paper confirm that while losses are independent of the network connectivity, a highly connected network will stabilize more quickly and with less oscillatory behavior. One measure that quantifies the lack of synchrony between network elements is that of "coherence" [16], which in the current context would be a measure of the variance of the deviation of network phases (averaged over the network) from what they ought to be in the absence of disturbances.

As expected, highly connected networks are more coherent than loosely connected ones, where connectivity here is a more subtle concept than node degree, but is rather related to the so-called spectral dimension of a network. We refer the reader to [16] for asymptotic scalings of lattice-type networks and to [17] for fractal networks, and note that these scalings are different than those that quantify network damping. One intuitive explanation for the cost of synchrony being independent of network topology is as follows. Comparing a highly connected network with a loosely connected one, we expect the former to have much more phase coherence than the latter. Consequently the power flows per link in a highly connected network are relatively small, but there are many more links than in the loosely connected network. Thus in the aggregate, the total power losses of the two networks are the same. One should keep in mind however, that a less coherent network is more likely to have transient stability problems, exit the region of attraction, etc. The issues of stability and the cost of synchrony are two different issues.

The remainder of this paper is organized as follows. Section II introduces the classical power system model and defines the notation. In Section III we quantify the total resistive line losses as an input-output H^2 norm of a linear dynamical system. This framework is then used to derive an algebraic expression for the resistive line losses in terms of the parameters of the admittance matrix, generator damping and the size of the network. Various interpretations of the H^2 norm are then presented together with the corresponding operating scenarios for a power network. The results of the analysis are demonstrated for two different network topologies in Section IV. Section V concludes the paper.

II. Problem Formulation

Consider a network of N buses (nodes) and $\mathcal{E}$ edges. At each node $i = 1, \ldots, N$ there is a generator G_i, with inertia constant M_i, damping β_i, voltage magnitude V_i and angle θ_i. Using the classic machine model the dynamics of the i^{th} generator is given by [18]

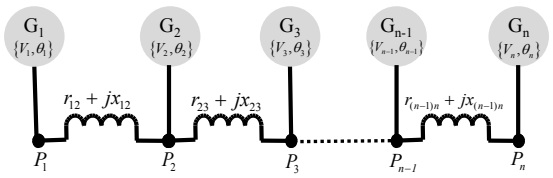

Fig. 1: A linear network of n generator nodes.

$$M_i\ddot{\theta}_i + \beta_i\dot{\theta}_i = P_{m,i} - P_{e,i} \qquad \forall\, i = 1, 2...n. \tag{1}$$

Here, $P_{e,i}$ is the electrical power output of the i^{th} generator, and $P_{m,i}$ is the mechanical power input from the turbine.

Define the admittance over edge $\mathcal{E}_{ij}$ connecting nodes i and j as $y_{ij} = g_{ij} - \mathbf{j}b_{ij}$, where g_{ij} and b_{ij} are respectively the conductance and susceptance of the line defined by the edge $\mathcal{E}_{ij}$. Then, the electrical power injection at node i is

$$\begin{aligned} P_{e,i} \;=\; & g_{ii}|V_i|^2 + \sum_{k\sim i} g_{ik}|V_i|\,|V_k|\cos(\theta_i - \theta_k) \\ & + \sum_{k\sim i} b_{ik}|V_i|\,|V_k|\sin(\theta_i - \theta_k), \end{aligned} \tag{2}$$

where $k \sim i$ denotes an edge $\mathcal{E}_{ik}$ and g_{ii} is the self admittance of the ith generator. In what follows, we use a simplified model where we assume $g_{ii} = \bar{g}$ for all $i = 1, \ldots, n$. Finally, applying the standard linear power flow assumptions used in transient stability analysis (conductances are negligible, angle differences are small and voltages are constant with unit magnitude) to (2) yields

$$P_{e,i} \approx \sum_{k\in\mathcal{N}} b_{ik}\left[\theta_i - \theta_k\right]. \tag{3}$$

Substituting this into (1) leads to

$$M_i\ddot{\theta}_i + \beta_i\dot{\theta}_i \approx -\sum_{k\in\mathcal{N}} b_{ik}\left[\theta_i - \theta_k\right] + P_{m,i}. \tag{4}$$

In order to simplify the notation we define the entries of the admittance matrix $Y \in \mathbb{C}^{n\times n}$ as

$$Y_{ij} := \begin{cases} \bar{g} + \sum_{j\sim i} y_{ij}, & \text{if } i = j, \\ -y_{ij}, & \text{if } i \neq j \text{ and } j \sim i, \text{ (i.e., } \mathcal{E}_{ij} \in \mathcal{E}), \\ 0 & \text{otherwise.} \end{cases}$$

Then, we partition this admittance matrix into the real (resistive) and imaginary (reactive) parts and define

$$Y \;=\; \mathrm{Re}\{Y\} \;+\; \mathbf{j}\;\mathrm{Im}\{Y\} \;=:\; (L_G + \bar{g}I) \;+\; \mathbf{j}\;L_B.$$

By this construction, L_G and L_B retain the symmetry of Y, and they have as a common eigenvector the vector $\mathbf{1}$ with components all equal to 1, i.e.

$$L_B\mathbf{1} \;=\; L_G\mathbf{1} \;=\; 0.$$

It is a well-known result that if the graphs underlying the system represented by L_B and L_G, which are analogous to weighted graph Laplacians, are connected (i.e. any two

nodes are connected by a path of edges), then the remaining eigenvalues of L_B and L_G are all positive.

An assumption we will invoke later is that all the eigenvectors of L_B and L_G are shared (u is an eigenvector of L_B iff it is an eigenvector of L_B). An important consequence of this assumption is that the two Laplacians are simultaneously diagonalizable by the same orthogonal transformation U, i.e.

$$U^* L_B U \;=\; \Lambda_B, \quad U^* L_G U \;=\; \Lambda_G, \tag{5}$$

where Λ_B and Λ_G are diagonal matrices with the respective eigenvalues of L_B and L_G as diagonal entries. One setting in which this assumption holds is when the ratios of each connection's conductance to susceptance (equivalently the ratios of resistances to reactances) are all equal, i.e.

$$\frac{g_{ik}}{b_{ik}} \;=\; \frac{r_{ik}}{x_{ik}} \;=\; \alpha,$$

which is independent of the link indices (i,k). It follows that

$$L_G \;=\; \alpha L_B, \tag{6}$$

which implies that L_G and L_B have the same eigenvectors.

Finally, we rewrite equation (4) in state space form

$$\begin{aligned} \frac{d}{dt}\begin{bmatrix}\theta(t)\\ \omega(t)\end{bmatrix} &= \begin{bmatrix}0 & I\\ -L_B & -\beta I\end{bmatrix}\begin{bmatrix}\theta(t)\\ \omega(t)\end{bmatrix} + \begin{bmatrix}0\\ I\end{bmatrix}\mathrm{w}, \quad (7)\\ &=: \; A\psi + B\mathrm{w}, \end{aligned}$$

where we have assumed that $M_i = 1$ for all i and that $P_{m,i}$ is constant and can be lumped into the input w.

Remark 1: Alternatively, the absence of $P_{m,i}$ in (7) can be justified as follows. For a system with no loads the equilibrium point of the system is at $P_{e,i} = P_{m,i}$. If (1) defines a linear system (as assumed here) a coordinate transform can be applied to obtain a new system with shifted angles θ^s corresponding to the transformed system with the equilibrium point $P_{m,i} = 0$. By abuse of notation we can denote the shifted coordinates as θ in (7).

Remark 2: The network model (7) represents a system of internal generator buses with loads approximated as impedances absorbed into the admittance matrix. The model could easily be extended to include static loads through a system of differential algebraic equations as in [13], [19].

III. System Performance

Several performance metrics can be used to quantify the relative stability for the system (7). For example, the ability to synchronize, the degree of synchronization that is achievable, the time to synchronize, or the control effort required to obtain a desired system state. In the distributed systems setting it is also common to evaluate these metrics with respect to various control strategies. For example, in evaluating the performance of a distributed system with local versus global control strategies. In this section we focus on the control actuation required to drive a system to the synchronous state. This control effort is measured through the real (resistive) power loss over each line. These losses are associated with circulating currents that arise from the angle differences between generators, i.e. disturbances [14].

The power flow over an edge $\mathcal{E}_{ij}$ is

$$P_{ij} + P_{ji} = V_i \left(V_i - V_j\right)^* y_{ij} + V_j \left(V_j - V_i\right)^* y_{ji},$$

where * denotes the complex conjugate. The resistive power loss over $\mathcal{E}_{ij}$ can therefore be defined as

$$P_{ik}^{loss} := g_{ik} \left|V_i - V_k\right|^2. \tag{8}$$

Using a small angle approximation and standard trigonometric identities this can be approximated as

$$\tilde{P}_{ik}^{loss} = g_{ik} \left|\theta_i - \theta_k\right|^2. \tag{9}$$

We are interested in the sum total of the resistive losses over all links in the network, which is given by

$$\tilde{\mathbf{P}}_{loss} = \sum_{i\sim k} g_{ik} \left|\theta_i - \theta_k\right|^2, \tag{10}$$

which can be expressed in vector form as $\tilde{\mathbf{P}}_{loss} = y^* y$. Here, the vector signal y is an output of (7)

$$y \;=\; C\psi \;=:\; \begin{bmatrix}C_1 & 0\end{bmatrix}\begin{bmatrix}\theta\\ \omega\end{bmatrix}, \quad \text{with } C_1^* C_1 := L_G. \tag{11}$$

Since L_G is positive semi-definite we can take $C_1 = L_G^{\frac{1}{2}}$, which is what we assume from now on.

We now calculate the H^2 norm from disturbance w to the performance output y of the system (7) and (11). The square of the H^2 norm has several standard interpretations including *(a)* The variance of the output y when the input w is a unit variance white stochastic process, *(b)* The total time integral of the variance of y when the initial condition is a random variable with correlation matrix BB^*, and *(c)* The total sum of time integrals of output response powers given an impulse as a disturbance input at each generator.

We first perform the H^2 norm calculation and derive a formula in terms of the system's parameters, and then investigate the implications of the three different interpretations for this particular system of swing equations.

H^2 Norm Calculation

For ease of reference we rewrite equations (7) and (11)

$$\begin{aligned} \tfrac{d}{dt}\begin{bmatrix}\theta\\ \omega\end{bmatrix} &= \begin{bmatrix}0 & I\\ -L_B & -\beta I\end{bmatrix}\begin{bmatrix}\theta\\ \omega\end{bmatrix} + \begin{bmatrix}0\\ I\end{bmatrix}\mathrm{w} \\ y &= \begin{bmatrix}L_G^{\frac{1}{2}} & 0\end{bmatrix}\begin{bmatrix}\theta\\ \omega\end{bmatrix} \end{aligned}. \tag{12}$$

We will denote the input-output mapping of this system by H. All eigenvalues of this system strictly in the left half of the complex plane with the exception of one zero eigenvalue of L_B. It is, however easy to show that this unstable mode is unobservable from the output y due to the fact that $L_G = C_1^* C_1$ shares this eigenvalue and its corresponding eigenvector (see Appendix for the full argument). It then follows that the input-output transfer function from w to y is indeed stable and has finite H^2 norm.

The H^2 norm of the (12) can be computed using a spectral decomposition of L_B. Consider the state transformation

$$\begin{bmatrix}\theta\\ \omega\end{bmatrix} \;=:\; \begin{bmatrix}U & 0\\ 0 & U\end{bmatrix}\begin{bmatrix}\hat{\theta}\\ \hat{\omega}\end{bmatrix},$$

where U is the matrix in (5) diagonalizing L_B and L_G. Since multiplying by orthogonal matrices does not change the H^2 norm, we can also define $\hat{\mathrm{w}} = U^*\mathrm{w}$ and $\hat{y} = U^*y$ to obtain an equivalent system (that has the same H^2 norm)

$$\begin{array}{rcl} \frac{d}{dt}\begin{bmatrix}\hat{\theta}\\ \hat{\omega}\end{bmatrix} & = & \begin{bmatrix}0 & I\\ -\Lambda_B & -\beta I\end{bmatrix}\begin{bmatrix}\hat{\theta}\\ \hat{\omega}\end{bmatrix} + \begin{bmatrix}0\\ I\end{bmatrix}\hat{\mathrm{w}} \\ \hat{y} & = & \begin{bmatrix}\Lambda_G^{\frac{1}{2}} & 0\end{bmatrix}\begin{bmatrix}\hat{\theta}\\ \hat{\omega}\end{bmatrix} \end{array}.$$

We will denote the input-output mapping of this system by $\hat{H}$. Since Λ_B and Λ_G are diagonal, this represents N decoupled systems

$$\begin{array}{rcl} \frac{d}{dt}\begin{bmatrix}\hat{\theta}_n\\ \hat{\omega}_n\end{bmatrix} & = & \begin{bmatrix}0 & 1\\ -\lambda_n^B & -\beta\end{bmatrix}\begin{bmatrix}\hat{\theta}_n\\ \hat{\omega}_n\end{bmatrix} + \begin{bmatrix}0\\ 1\end{bmatrix}\hat{\mathrm{w}}_n \\ \hat{y}_n & = & \begin{bmatrix}\sqrt{\lambda_n^G} & 0\end{bmatrix}\begin{bmatrix}\hat{\theta}_n\\ \hat{\omega}_n\end{bmatrix} \end{array},$$

where $n = 1, \ldots, N$ are the indices of eigenvalues λ_n^B and λ_n^G, which correspond to L_B and L_G respectively. Denote the input-output mapping of each decoupled subsystem by $\hat{H}_n$. We can then write $\hat{H} = \mathrm{diag}\left(\hat{H}_1, \ldots, \hat{H}_N\right)$.

The square of the H^2 norm of (12) is the sum of the squares of the H^2 norms of all the decoupled subsystems

$$\|H\|_2^2 = \|\hat{H}\|_2^2 = \sum_{n=1}^{N} \|\hat{H}_n\|_2^2.$$

The H^2 norm of each of the individual subsystems can now be easily calculated as follows. For $n = 1$, the corresponding eigenvalues are $\lambda_1^B = \lambda_1^G = 0$, and we have a completely unobservable system, thus $\|\hat{H}_1\|_2 = 0$. For $n \neq 1$, we solve the Lyapunov equation for the observability Grammians $\hat{X}_n$

$$\begin{array}{rcl} \begin{bmatrix}0 & -\lambda_n^B\\ 1 & -\beta\end{bmatrix}\begin{bmatrix}\hat{X}_{11} & \hat{X}_0\\ \hat{X}_0^* & \hat{X}_{22}\end{bmatrix} + \begin{bmatrix}\hat{X}_{11} & \hat{X}_0\\ \hat{X}_0^* & \hat{X}_{22}\end{bmatrix}\begin{bmatrix}0 & 1\\ -\lambda_n^B & -\beta\end{bmatrix} & & \\ = -\begin{bmatrix}\lambda_n^G & 0\\ 0 & 0\end{bmatrix}, & & \end{array}$$

where for simplicity of notation we omit the subscript n from the components of $\hat{X}_n$. This matrix equation corresponds to three equations, of which only the following two are relevant

$$\begin{array}{ll} -\lambda_n^B\hat{X}_0^* - \hat{X}_0\lambda_n^B = -\lambda_n^G & \Rightarrow \mathrm{Re}(\hat{\mathrm{X}}_0) = \frac{1}{2}\frac{\lambda_{\mathrm{n}}^{\mathrm{G}}}{\lambda_{\mathrm{n}}^{\mathrm{B}}} \\ \hat{X}_0 + \hat{X}_0^* - 2\beta\hat{X}_{22} = 0 & \Rightarrow \hat{X}_{22} = \frac{1}{\beta}\mathrm{Re}(\hat{\mathrm{X}}_0). \end{array}$$

Finally, since the B matrix of each subsystem is $[0\ 1]^T$, the H^2 norm (squared) of each subsystem is just $\hat{X}_{22}$, thus

$$\|\hat{H}_n\|_2^2 = \frac{1}{2\beta}\frac{\lambda_n^G}{\lambda_n^B}.$$

Thus the total H^2 norm (squared) of the system (12) is

$$\|H\|_2^2 = \frac{1}{2\beta}\sum_{n=2}^{N}\frac{\lambda_n^G}{\lambda_n^B} = \frac{1}{2\beta}\sum_{n=2}^{N}\frac{\alpha\lambda_n^B}{\lambda_n^B} = \frac{\alpha}{2\beta}(N-1).$$

In summary, we conclude that the total resistive losses are

$$\boxed{\|H\|_2^2 = \frac{1}{2\beta}\frac{r}{x}(N-1),} \tag{13}$$

where β is a generator's self damping, $\frac{r}{x}$ is the ratio of a line's resistance to its reactance (assumed equal for all lines), and N is the number of generators in the network. In practice, power grids are designed to minimize real power losses, so $\frac{r}{x}$ is small and r is often neglected in power flow calculations [15] as in (3). The result (13) shows that increasing the number of generators will increase these losses, regardless of the network topology a fact that will become increasingly important as generation becomes more distributed.

H^2 Norm Interpretations for Swing Dynamics

In the previous subsection we calculated the H^2 norm of the linearized swing dynamics (7), together with the output equation (11) based on a disturbance input (forcing) w. In our formulation the square of the Euclidean norm y^*y of the output vector was defined to be equal to the total real power dissipated due to resistive losses in the network connections as the system synchronized. This synchronized state (the equilibrium) is maintained by circulating currents leading to power flowing back and forth between generator nodes.

It is well known that the H^2 norm has at least three different interpretations, which we recall here to provide different physical scenarios in which equation (13) quantifies the resistive losses due to the synchrony requirement. Denote by H the following Linear Time Invariant (LTI) system

$$\begin{array}{rcl} \dot{\psi}(t) & = & A\psi(t) + B\mathrm{w}(t) \\ y(t) & = & C\psi(t), \end{array}$$

The H^2 norm of the system can be interpreted as follows.

(a) *Response to a white stochastic input.* When the input w is a white second order process with unit covariance (i.e. $E\{\mathrm{w}(t)\mathrm{w}^*(t)\} = I$), the H^2 norm (squared) of the system is the steady-state total variance of all the output components, i.e.

$$\|H\|_2^2 = \lim_{t\to\infty} E\{y^*(t)y(t)\}.$$

For the swing dynamics (12) the disturbance vector can be thought of as persistent stochastic forcing at each generator. These disturbances, which are uncorrelated across generators, can be due to uncertainties in local generator conditions, sudden changes in load, or fault events. The variance of the output is exactly the expectation of the total power loss due to line resistances.

(b) *Response to a random initial condition.* With zero input and an initial condition that is a random variable x_o with correlation $E\{x_o x_o^*\} = BB^*$, then the H^2 norm is the time integral

$$\|H\|_2^2 = \int_0^\infty E\{y^*(t)y(t)\}\ dt$$

of the resulting response y.

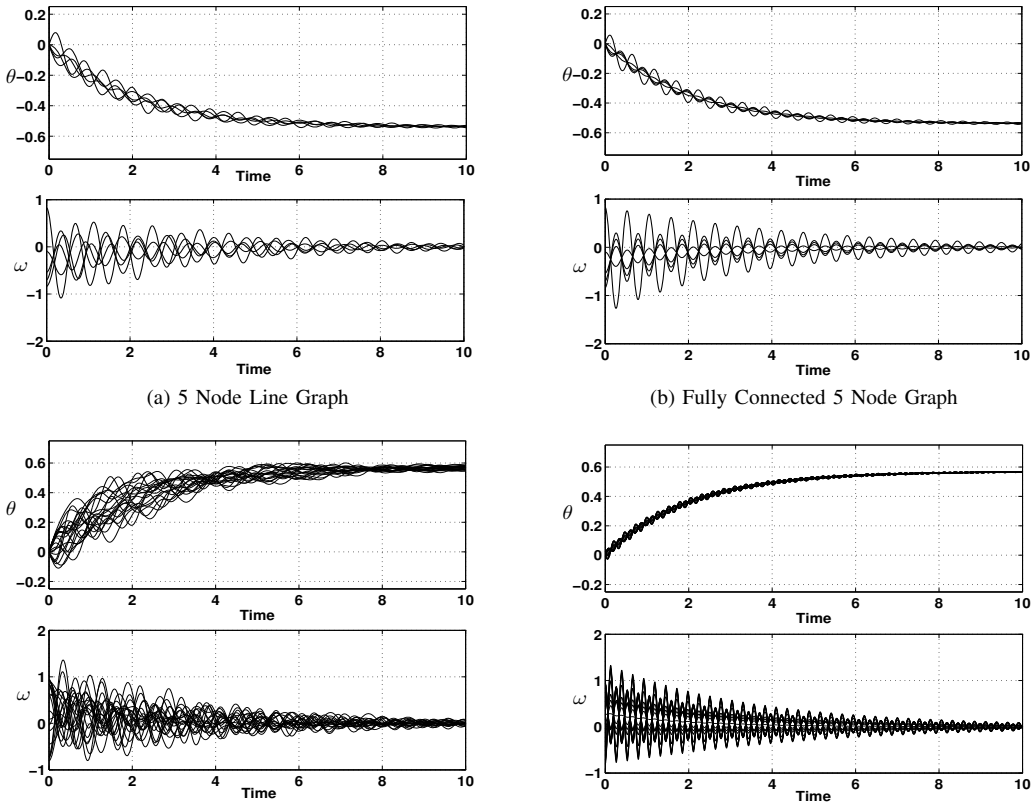

(a) 5 Node Line Graph

(b) Fully Connected 5 Node Graph

(c) 20 Node Line Graph

(d) Fully Connected 20 Node Graph

Fig. 2: (a),(b) Simulation of a 5 bus system of identical oscillators random velocity and zero phase initial conditions. (c),(d) Simulation of a system with 20 identical oscillators under the same conditions as in (a),(b). Figures (a),(c) are for linearly connected networks (with line graphs as in Figure 1), while Figures (b),(d) are for fully connected networks (complete graphs). The linear networks are less coherent than complete networks (Figures (a),(c) versus (b),(d) respectively).

The interpretation for (12) is as follows. Since $BB^* = \begin{bmatrix} 0 & 0 \\ 0 & I \end{bmatrix}$, the corresponding initial condition corresponds to each generator having a random initial velocity perturbation that is uncorrelated across generators and zero initial phase perturbation. Then $\|H\|_2^2$ quantifies the total (over all time) expected resistive power losses due to the system returning to a synchronized state.

(c) *Sum of responses to impulses at all inputs.* Let e_i refer to the vector with all components zero expect for 1 in the i^{th} component. Consider N experiments where in each, the system is fed an impulse at the i^{th} input channel, i.e. $\mathrm{w_i(t)} = \mathrm{e_i}\delta(\mathrm{t})$. Denote the corresponding output by y_i. The H^2 norm (squared) is then the sum total of the L^2 norms of these outputs, i.e.

$$\|H\|_2^2 \;=\; \sum_{i=1}^{N} \int_0^\infty y_i^*(t) y_i(t)\; dt.$$

A stochastic version of this scenario corresponds to a system where the inputs $\mathrm{w_i}$ can occur with equal probability. Under this assumption the $\|H\|_2^2$ becomes the expected total power loss given these inputs.

The corresponding interpretation for (12) is when each generator is subject to impulse force disturbances (since w enters into the momentum equation of each generator), and $\|H\|_2^2$ is then the total power loss over all time.

IV. Numerical Examples

Consider two networks of identical generators, one whose underlying graph is a line, as in Figure 1, and one with a fully connected graph. In this section, we compare the behavior of two such systems as the network size varies. All simulations use the following parameter values [20]: $M = \frac{20}{2\pi f}$, $\beta = \frac{10}{2\pi f}$ with a frequency $f = 60$ Hz. The admittance between connected generators is set to $y_{ij} = 0.2 + \mathbf{j}1.5$ and we assume $g_{ii} =: \bar{g} = 0$ for all $i = 1, \ldots, n$.

Figures 2a and 2b respectively show the state trajectories of a 5 node system with a line graph and one with a fully connected graph given identical initial conditions. The initial conditions for each $\omega_i(0)$ were drawn from a uniform distribution $[-1, 1]$, and $\theta(0)$ was set to zero. This corresponds to the H^2 norm interpretation (b) described in the previous section. For both the line graph and the fully connected network the total losses are the same, with

$\mathbf{P}^{loss} = 1.2885$, as predicted by the main result in (13). However, the transient behavior shows that the system with the fully connected graph has more "coherent" phases (i.e. they stay closer together). This is most clearly visible in the top panels of the plots that depict the state θ. Here, the small oscillations for the line graph system continue through the 10 second interval shown in Figure 2a but have almost completely died out for the fully connected of Figure 2b.

In order to evaluate the effect of increasing the network size we ran a similar test with two 20 bus systems with the same topological structure and initial conditions ($\omega_i(0) \in [-1, 1]$ drawn from a uniform distribution for each i and $\theta(0) = 0$). In this case, the losses increased to $\mathbf{P}^{loss} = 5.9256$ but remained equal in both networks. The faster convergence to the synchronized state in fully connected system (compared to the line graph) is much more evident in the larger network, as shown in figures 2c and 2d.

The simulation results indicate that a fully connected graph is much more coherent than a line graph. The resemblance of this result to those about coherence in vehicular formations (platoons) and similar consensus-like network algorithms [16] is striking. With coherence as a performance measure, the line graph is the worst such topology (amongst connected graphs), while the fully connected topology is the best. However this additional coherence, while desirable for other reasons, will not result in lower resistive losses.

V. Conclusions

We have considered a power network model with distributed disturbances, and quantified the total resistive power losses incurred due to the current flows needed to maintain phase synchrony. We have shown that these losses are independent of the network's topology, but scale unboundedly with the number of generators. There are interesting implications for the design of future highly-distributed-generation networks, which have potentially orders of magnitude more generator nodes that today's networks. While a highly phase coherent (and therefore highly connected) network is desirable for many reasons, the cost of maintaining this coherence depends only on the number of generators and not the network's connectivity. Since this cost grows unboundedly with the number of generator nodes, then the current scheme of using power flows as the synchronization mechanism may not be scalable to future networks. This is perhaps a further argument for the use of other control mechanisms, such as communication links, for phase synchronization.

Appendix

Proof that (12) *is input-output stable*

It is well known that for any pair (C, A), the observability of (C, A) and (C^*C, A) are equivalent. The only unstable mode of the A-matrix in (12) is at zero with corresponding eigenvector $[\mathbf{1}, 0]^T$. This mode is unobservable from the output y since by the PBH test

$$\begin{bmatrix} -A \\ C^*C \end{bmatrix} \begin{bmatrix} \mathbf{1} \\ 0 \end{bmatrix} = \begin{bmatrix} \begin{bmatrix} 0 & -I \\ L_B & \beta I \end{bmatrix} \\ \begin{bmatrix} L_G & 0 \\ 0 & 0 \end{bmatrix} \end{bmatrix} \begin{bmatrix} \mathbf{1} \\ 0 \end{bmatrix} = \begin{bmatrix} 0 \\ 0 \end{bmatrix}.$$

Note that this is a consequence of L_G and L_B having the common eigenvector $\mathbf{1}$ with eigenvalue 0. The unobservability of the only unstable mode implies then that the system (12) is input-output stable.

References

[1] U.S. Energy Information Administration, "Annual energy outlooks 2010 with projections to 2035," U.S. Dept. of Energy, Tech. Rep. DOE/EIA-0383, 2010.

[2] J. Carrasco et al., "Power-electronic systems for the grid integration of renewable energy sources: A survey," *IEEE Trans. on Industrial Electronics*, vol. 53, no. 4, pp. 1002–1016, 2006.

[3] V.S. Budhraja et al., "California's electricity generation and transmission interconnection needs under alternative scenarios," California Energy Commission, Tech. Rep., 2004.

[4] P. Kundur et al., "Definition and classification of power system stability IEEE/CIGRE joint task force on stability terms and definitions," *IEEE Trans. on Power Sys.*, vol. 19, no. 3, pp. 1387 – 1401, Aug. 2004.

[5] P. Varaiya, F. Wu, and R.-L. Chen, "Direct methods for transient stability analysis of power systems: Recent results," *Proc. of the IEEE*, vol. 73, no. 12, pp. 1703 – 1715, Dec. 1985.

[6] L. F. C. Alberto, F. H. J. R. Silva, and N. G. Bretas, "Direct methods for transient stability analysis in power systems: state of art and future perspectives," in *IEEE Power Tech Proc.*, vol. 2, Porto, Portugal, 2001.

[7] L. Pecora and T. Carroll, "On the existence of energy function for power systems with transmission losses," *Phys. Rev. Letters*, vol. 80, no. 10, pp. 2109–2112, 1998.

[8] N. Narasimhamurthi, "On the existence of energy function for power systems with transmission losses," *IEEE Trans. on Circuits and Sys.*, vol. 31, no. 2, pp. 199 – 203, Feb. 1984.

[9] H.-D. Chiang, F. Wu, and P. Varaiya, "Foundations of the potential energy boundary surface method for power system transient stability analysis," *IEEE Trans. on Circuits and Sys.*, vol. 35, no. 6, pp. 712 –728, June 1988.

[10] F. H. J. R. Silva, L. F. C. Alberto, J. B. A. London Jr., and N. G. Bretas, "Smooth perturbation on a classical energy function for lossy power system stability analysis," *IEEE Trans. on Circuits and Sys. I*, vol. 52, no. 1, pp. 222 – 229, Jan. 2005.

[11] F. Dörfler and F. Bullo, "Synchronization and transient stability in power networks and non-uniform Kuramoto oscillators," in *Proc. of the American Control Conf.*, Baltimore, MD, 2010, pp. 930 –937.

[12] ——, "Topological equivalence of a structure-preserving power network model and a non-uniform Kuramoto model of coupled oscillators," in *Proc. of IEEE Conf. on Decision and Control*, Orlando, FL, 2011, pp. 7099 –7104.

[13] E. Mallada and A. Tang, "Improving damping of power networks: Power scheduling and impedance adaptation," in *Proc. of the IEEE Conf. on Decision and Control*, Orlando, FL, 2011, pp. 7729 – 7734.

[14] A. von Meier, *Electric Power Systems: A Conceptual Introduction*, E. Desurvire, Ed. Hoboken, NJ: John Wiley and Sons Inc., 2006.

[15] K. Purchala et al., "Usefulness of DC power flow for active power flow analysis," in *Proc. of IEEE PES Gen. Meeting*, 2005, pp. 2457–2462.

[16] B. Bamieh, M. R. Jovanovic, P. Mitra, and S. Patterson, "Coherence in large-scale networks: Dimension-dependent limitations of local feedback," *IEEE Trans. on Automatic Control*, vol. 57, no. 9, pp. 2235 –2249, Sept. 2012.

[17] S. Patterson and B. Bamieh, "Network coherence in fractal graphs," in *Proc. of the IEEE Conf. on Decision and Control*, Orlando, FL, 2011, pp. 6445–6450.

[18] M. A. Pai, *Power System Stability by Lyapunov's Method*. New York, NY: N.Holland Publishing Co., 1981.

[19] D. Hill and G. Chen, "Power systems as dynamic networks," in *Proc. of the IEEE Int'l Symposium on Circuits and Sys.*, 2006, pp. 722–725.

[20] P. Sauer and M. A. Pai, Eds., *Power System Dynamics and Stability*. Upper Saddle River, NJ: Prentice Hall, 1999.